Measurement Of Ultrafast Ionisation From Intense Laser Interactions With Gas-Jets

Leonida A. GIZZI*, Marco GALIMBERTI*, Antonio GIULIETTI, Danilo GIULIETTI*, Petra KOESTER, Luca LABATE*, Paolo TOMASSINI*

Intense Laser Irradiation Lab., IPCF, Area della Ricerca CNR, Via Moruzzi, 1 56124 Pisa, Italy
**Also at Istituto Nazionale Fisica Nucleare – INFN, Pisa, Italy*

Philippe MARTIN, Tiberio CECCOTTI, Pascal DE OLIVEIRA, Pascal MONOT

Physique à Haute Intensité, CEA-DSM/DRECAM/SPAM, Bât. 522 p. 148, 91191 Gif sur Yvette Cedex, FRANCE

Abstract. Interaction of an intense, ultrashort laser pulse with a gas-jet target is investigated through femtosecond optical interferometry to study the dynamics of ionization of the gas. Experimental results are presented in which the propagation of the pulse in the gas and the consequent plasma formation is followed step by step with high temporal and spatial resolution. We demonstrate that, combining the phase shift with the measurable depletion of fringe visibility associated with the transient change of refractive index in the ionizing region and taking into account probe travel time can provide direct information on gas ionization dynamics.

Keywords: Ultrafast ionization, propagation, optical probing.
PACS: 52.50.Jm, 52.25.Jm, 52.70.Kz

INTRODUCTION

The interaction of intense femtosecond Chirped Pulse Amplification[1] (CPA) laser pulses with gases is extensively exploited for the investigation of a wide range of phenomena in both fundamental and applied sciences. In fact, laser interaction with gas-jets is now regarded as the most promising framework for the achievement of laser-driven acceleration of charged particles [2]. On the other hand, schemes for the generation of ultra-short pulses of radiation from the UV [3] to the X-ray range [4] also rely upon this class of interaction experiments. From a more fundamental viewpoint, interaction of intense laser fields with gas-jets is a primary tool for the investigation of fundamental ionization issues and can be used to benchmark models of high-field ionization [5].

Investigation of the ionization dynamics can be carried out using optical spectroscopy to infer ionization rates from the detection of a blue-shift of either the

CP827, *Superstrong Fields in Plasmas: Third International Conference on Superstrong Fields in Plasmas*, edited by D. Batani and M. Lontano

interacting pulse or a suitably delayed probe pulse [6] and [7]. In this case, the evolution of the intensity and phase of the input laser pulse will affect the properties of the blue-shifted light, therefore, additional information is required for a complete description of the ionization dynamics. These complications have been successfully overcome by using frequency resolved optical gating [8] which was demonstrated to provide reliable quantitative measurements of ionization dynamics.

Well-established optical probe interferometry can give information on ionized gas regions at the sub-micron scale. In fact, interferometry is a well known tool for the 2-D mapping of plasma density in a variety of geometrical and physical configurations, from the exploding foil technique [9] to the characterization of plasma precursor effects in interaction of CPA pulses with solids [10]. Also, provided a sufficiently short probe pulse is used, plasma electron density can be mapped on a fs time scale using a pump and probe-like approach. Similar techniques have already been successfully applied to time-resolving several phenomena including, for example, channel formation in gas-jets [11] or radiative blast waves [12].

While being in principle a simple and relatively easy technique to implement in the case of relatively long probe pulses, its use for the investigation of ultra-fast ionization dynamics has been limited. In fact, in this class of experiments, time resolution on the femtosecond time-scale is required. In these circumstances, visibility of a large number of fringes required to obtain an interferogram can be affected by the very short probe pulse duration. Recently, the use of a well-known scheme for laser-plasma interferometry, the so-called modified Nomarski interferometry [13], has been successfully demonstrated [10] using a frequency doubled CPA femtosecond pulse to probe plasma density during laser-driven electron acceleration experiments. In that case, interferometry was used to measure the density profile of the plasma generated by the Amplified Spontaneous Emission (ASE) just before the arrival of the main CPA pulse. The use of very short probe pulse was necessary to prevent loss of fringe visibility due to plasma motion arising from ASE induced heating. Some information concerning the propagation of the CPA pulse in the preformed plasma could also be gained from closely (temporally) spaced interferograms in a pump and probe approach. However, the poor reproducibility of background plasma conditions from shot to shot did not enable accurate measurements of CPA induced ionization and propagation issues.

In this work we show for the first time that short pulse optical probing interferometry can be successfully applied to a quantitative investigation of ionization dynamics on the femtosecond time-scale and on the micrometer-scale spatial resolution. Our measurements enabled us to follow the propagation of an expanding CPA pulse in a gas-jet through the time-resolved measurement of the density map. The temporal resolution enabled us to follow the ionization front from the focal region, where the intensity is well above the ionization threshold, to the expanded region, where local intensity goes below the ionization threshold. We show that localized ionization of the gas due to the CPA pulse induces a detectable partial depletion of fringe visibility (FVD) associated with the transient change of refractive index in the ionizing region. We demonstrate that, combining this FVD with standard phase shift information and taking into account probe travel time in the interaction region can be used to obtain a quantitative information of ionization dynamics on the

femtosecond time-scale and on the micrometer-scale spatial resolution. To our knowledge, this is the first experiment in this field in phase shift and fringe visibility of interferometry maps are taken into account simultaneously.

EXPERIMENTAL SET UP

The experiment was performed at the SLIC laser facility at the Saclay Centre of CEA (France) with the 10 TW UHI10 laser system. The Ti:Sa laser system operates in the CPA mode and delivers up to 0.6 J in 60-fs laser pulses at 800-nm. The contrast of the main laser pulse on both the nanosecond and picosecond scale were measured by a third order auto-correlator. The nanosecond contrast, due to Amplified Spontaneous Emission (ASE), was found to start about 1ns before the main pulse with a contrast ratio of $\approx 10^{-6}$, while the *pedestal* of the femtosecond pulse, due to the pulse compression, had a contrast ratio of $\approx 10^{-4}$ for a duration of about 1ps before the main pulse. These values are typical of most high power femtosecond lasers.

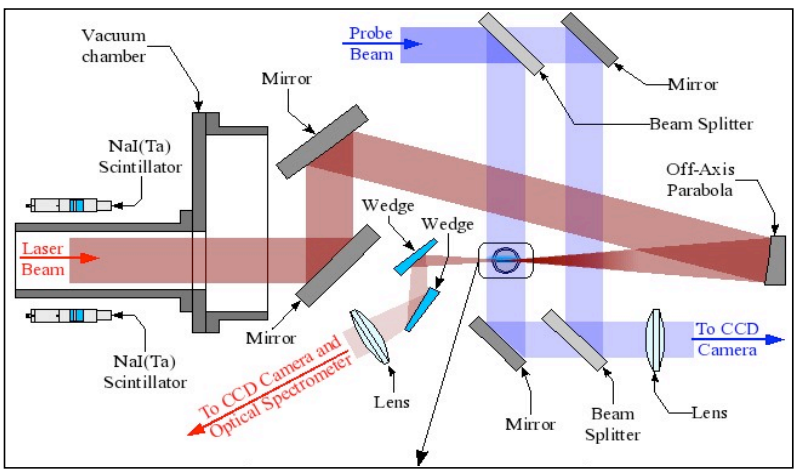

Figure 1. Schematic experimental set up showing the main diagnostics including the interferometer, the optical spectrometers and the γ-ray detectors.

A schematic view of the experimental set up is shown in Figure 1. The pulse was focused in the gas jet using a 200 mm, silver coated off-axis parabolic mirror. The numerical aperture of the focusing optics was f/2.5 and the maximum focused nominal intensity was 10^{19} Wcm^{-2} in a slightly elliptical focal spot whose horizontal and vertical diameters were 8μm and 10μm FWHM respectively. The corresponding normalised field parameter in the focal spot was $a_o = 2.6$.

A fraction of the main femtosecond pulse was frequency-doubled using a 3 mm thick, type I KDP (Potassium Dihydrogen Phosphate) crystal and used as an optical probe propagating perpendicular to the main pulse, in a Mach-Zehnder interferometer configuration. The probe pulse is expected to have a pulse duration of approximately 240 fs, due to group velocity dispersion in the 3mm frequency doubling crystal. The

optical configuration was optimised in terms of field of view, spatial resolution and signal-to noise ratio.

The gas-jet was delivered by a 1 mm diameter, cylindrical nozzle. The He_2 gas pressure in the valve was 8 bar and the maximum neutral density was greater than 10^{19} atoms/cm^{-3}. A phase shift map due to the neutral He gas is shown in Figure 2. The map was obtained from a Fourier analysis [14,9] of the fringe pattern taken with the Mach-Zehnder interferometer. According to this map, the maximum phase shift is detected on the axis of the nozzle and corresponds to approximately one third of a wavelength of the probe beam. The jet is visible up to the boundary where the phase shift is as small as one tenth of a wavelength.

The arrow indicates the direction of propagation of the CPA pulse, set to propagate along a diameter of the nozzle, at a distance of 200 μm from the nozzle edge. The best focus was at the boundary of the jet, at a distance of 870 μm from the nozzle axis. At this distance the gas density was found to be sufficiently low so as to prevent precursor plasma formation by the Amplified Spontaneous Emission. This enabled us to investigate the effect of CPA interaction with the neutral gas, without nanosecond-scale preformed plasma.

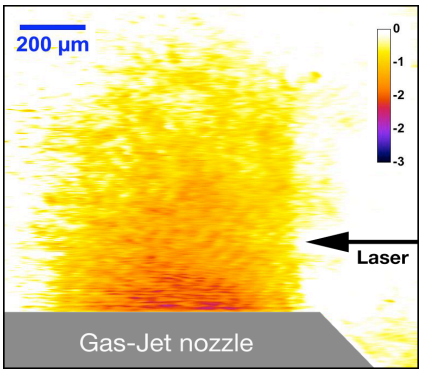

Figure 2. Phase-shift map due to neutral He gas at a valve gas pressure of 8 bar. The nozzle was cylindrical with a 1mm diameter. The maximum phase shift is detected on the axis of the nozzle and corresponds to less than half of a wavelength of the probe beam. The arrow indicates the direction of propagation of the main CPA pulse. The best focus is located at 870 μm from the nozzle axis.

The history of the ionization of the gas following propagation of the CPA pulse was measured in a "pump and probe"-like approach, by taking a series of interferograms by varying the delay between the probe pulse to main pulse shot by shot with a time step as small of 330 fs. As mentioned above, the control of the position of the best focus enabled us to prevent the ASE effect allowing the ionization of the gas to be followed during the whole transit of the CPA pulse, in a sequence of closely (temporally) spaced frames. This control was necessary to obtain a high level of reproducibility of the interaction dynamics, a prerequisite for a meaningful pump and probe investigation. In fact, in the case of interaction conditions dominated by the effect of ASE, we found that the precursor plasma was characterised by a size and the scale-length that was changing from shot-to-shot, with a consequent poor reproducibility.

OVERVIEW OF DATA

The image of Figure 3 shows an interferogram taken at probe time +2.33 ps, where probe time zero is conventionally defined as the time at which the CPA pulse reaches the best focus position of the optics. The plot in the same figure shows the average laser intensity of the main CPA pulse as it propagates across the plasma. According to this plot we find that the laser intensity has a maximum of 1.5×10^{19} W/cm^2 in the best focus and decreases up to 10^{17} W/cm^2 at a distance of 600μm. Therefore we can assume that, up to this distance from the best focus, the laser intensity is above the level required for a full ionisation of Helium [15]. Beyond this point, the actual intensity distribution in the beam must be taken into account. In fact, as the beam propagates, the intensity decreases and, starting from the wings, will go below the level required to produce a detectable density of free electrons. For this reason we expect that the transverse size of ionised region will get smaller around the beam axis.

At the probe time of Figure 3, the pump pulse has well passed the best focus position and the fringe shift pattern still show a cone-like shape with an aperture of approximately 25 deg. We observe that this aperture corresponds to the full aperture of the focusing optics as indicated by the solid line that marks the $1/e^2$ profile of the beam, assuming Gaussian propagation for an f/2.5 beam.

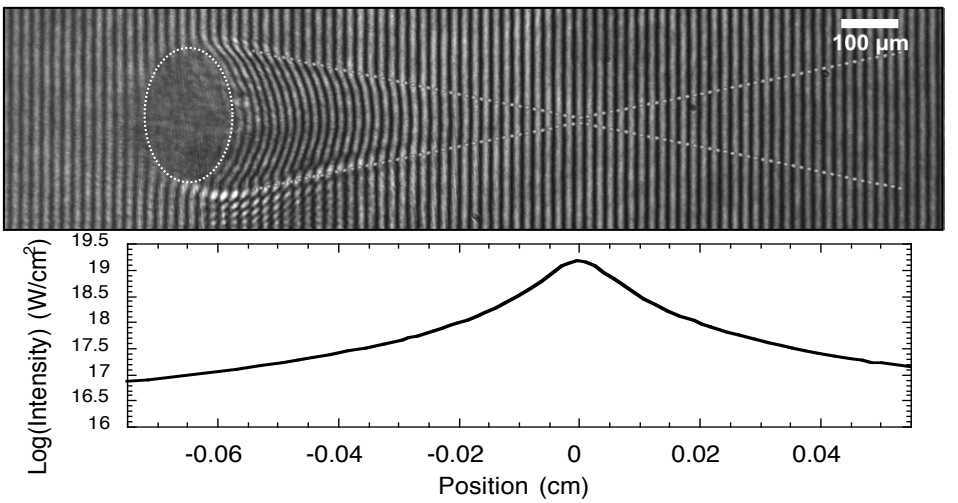

Figure 3. Interferogram of laser propagation in He (8 bars) taken at T=+2.33ps. The laser pulse propagates from right to left and the line shows the $1/e^2$ profile of the incident beam, focused with an f/2.5 optics. The dotted ellipse shows the region where temporary loss of fringe visibility occurs. The plot shows the dependence of the average laser intensity along the laser propagation axis.

The distance between the leading edge and the best focus position is approximately 780μm. This value is in a good agreement with the value expected for a propagation at the speed of light starting from the position of the best focus at probe time zero. This behaviour is summarised by the plot of Figure 4 where the position of the leading edge as taken from each probe frame is plotted as a function of the probe time delay. Up to probe time 3ps, the leading edge proceeds at the speed of light as indicated by the

linear fit. Beyond that point, the position of the fringe perturbation front apparently slows down and no further propagation is detected after 3.67 ps. At this time the CPA pulse has propagated for 1.2 mm beyond the best focus and the nominal laser intensity is 1.6×10^{15} W/cm^2. Beyond this point, no significant fringe perturbation occurs and, taking into account the geometry of the beam propagation and the interferometer sensitivity, the electron density in this region must be smaller than 10^{17} cm^{-3}.

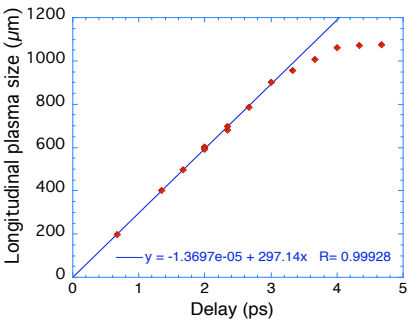

Figure 4. Position of the leading edge of the perturbed fringe region as a function of the probe delay time. Probe time zero is conventionally set at the time of arrival of the main pulse at the best focus. The solid line is the linear fit to the data points up to delay time 3ps.

The actual electron density map as obtained from the analysis of a portion of the interferogram of Figure 3 is shown in Figure 5. In this case, a generalised Abel inversion algorithm [16] was used to account for moderate deviation from the cylindrical symmetry. In fact, the background gas density decreases as a function of the distance from the nozzle as clearly shown in the map of Figure 2. Our inversion technique accounts partially for this effect, showing a non axi-symmetric electron density map.

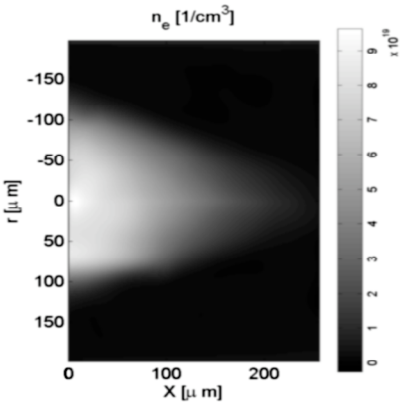

Figure 5. Electron density map as obtained from the analysis of the interferogram of Figure 3, applying a generalized Abel inversion algorithm that accounts for moderate deviations from cylindrical symmetry.

An important feature of our interferograms is the significant loss of fringe visibility just behind the leading edge of the plasma region, as marked by the dotted ellipse in the interferogram of Figure 3. In other words, the amplitude of the intensity modulation associated with the fringe pattern decreases in this region. This feature is very reproducible and only occurs during the transit of the pulse in the region where significant ionisation occurs. Also, this loss of fringe visibility is highly transient and, as discussed below, moves ahead with the laser pulse. A detailed analysis of this fringe visibility issue is given in the following section.

FRINGE VISIBILITY

A quantitative analysis of the fringe visibility can be carried out from interferometry maps using the Fourier transform analysis applied to extract phase maps as discussed in detail in [9]. In fact, it can be shown that the Fourier transform analysis of digitised fringe maps yields a complex array. The imaginary part of this array gives the phase map while the real part of the array gives the amplitude, namely the visibility of the fringes. The image of Figure 6 shows the visibility map of the same interferogram of Figure 3, taken at +2.3ps.

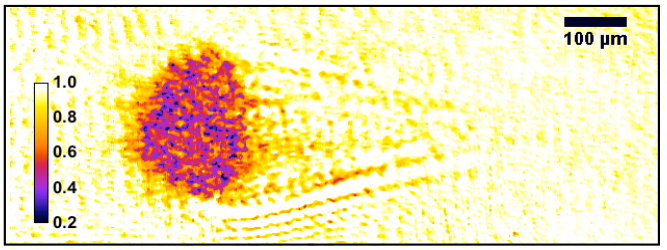

Figure 6. Map of fringe visibility obtained from Fourier analysis of the same interferogram shown in Figure 3. Laser pulse propagates from right to left. The map shows a well defined region of significant loss of fringe visibility. Minor perturbations to the fringe pattern, due to diffraction, are also visible at the boundaries of the plasma.

A well defined region of significant loss of fringe visibility (Fringe Visibility Depletion, FVD) is clearly visible in the map, along with some minor modulations of the fringe visibility at the upper and lower boundary of the plasma due to diffraction. According to this map, the region of low visibility has a longitudinal width of approximately 165µm and a transverse width of 230 µm (FWHM).

The analysis of the entire history of propagation shows that a region of poor fringe visibility appears as early probe time 1.34ps. At this time the transverse size of the low visibility region is 110µm and the longitudinal size is 90µm. Similar maps can be obtained for all the interferograms taken at different times. The plots of Figure 7 show the lineouts of the visibility maps similar to the one of Figure 6 for interferograms taken from probe time 1ps to probe time 3 ps with inter-frame time of 330 fs.

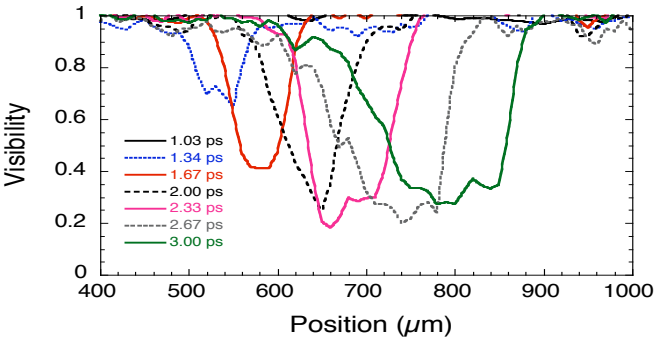

Figure 7. Longitudinal profiles of fringe visibility taken on the laser propagation axis integrated over a 32μm transverse width. The laser propagates from left to right. Each curve shows the fringe visibility at each probe time and normalized to the unperturbed fringe visibility.

Lineouts were taken on the laser propagation axis integrating on a 32 μm wide slice. Plots are normalised to the corresponding values of the unperturbed fringe pattern. According to these plots, the loss of visibility at a given probe time, exhibits a weakly flat-top profile with a top level increasing gradually from approximately 20% to approximately 50% loss with respect to the unperturbed visibility value.

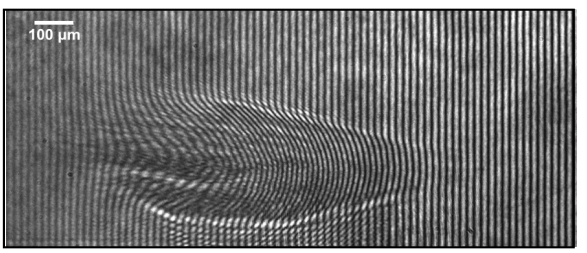

Figure 8. Fringe pattern taken at probe time +4.67 ps. The laser pulse propagates from right to left as shown by the dashed lines of Figure 5.

Also, the FWHM of each curve increases from approximately 100 μm at 1.34 ps to more than 260 μm at 3 ps At times later than 3 ps visibility is rapidly restored and at probe time +4.67 ps almost full recovery of fringes occurs as clearly shown in the raw interferometry map of Figure 8. Beyond this time, interferograms show a clear fringe pattern varying very slowly on a ns time-scale.

INTERPRETING LOSS OF VISIBILITY

In general, several factors can lead to a loss of fringe visibility in interferometric measurements like those presented here. The probe pulse can be partially or totally absorbed in the probed plasma. In the worst case, only the reference beam reaches the image plane of the interferometer producing no interference pattern in the regions where absorption of the probe has taken place. In addition, steep plasma gradients transverse to the probe propagation direction can deflect the probe beam outside the

collecting cone of the imaging optics of the interferometer. Again, the image plane shows no fringes in the region of the plasma where strong refraction has occurred.

We point out that, in both cases, the intensity in the FVD region at the probe image plane is expected to be equal to the intensity of the reference beam. Another feature of both these processes is their slow recovery time. In fact, once they have been established (e.g. by ionisation), changes in the plasma absorption and refraction will evolve on the time-scale of plasma hydrodynamics.

In our case, considering the typical plasma density and temperatures, hydrodynamic evolution can be expected to occur on the nanosecond time-scale. In contrast, our measurements show a is highly transient behaviour, with almost full recovery of fringe visibility on the femtosecond time-scale. Also, the intensity in the FVD region is very close to the value of twice the intensity of each interfering beam, as expected in the case of no or negligible loss of probe beam intensity. According to these considerations, absorption and refraction can only give a marginal contribution to the observed FVD.

The observed features can be explained by taking into account a third possible source of FVD, namely the transient change of the refractive index of the plasma during probe pulse. In fact, if the change of refractive index during the probe pulse is sufficiently fast, a sizeable change of the optical path will take place during the probe pulse. If this change is a significant fraction of the probe wavelength, λ_p, fringe motion occurs with consequent smearing of the fringe pattern in the region affected by this process.

We assume that the change of refractive index arises from a change of plasma density due to ionisation of the gas by interaction with the main CPA pulse. As the pulse propagates, field ionisation occurs very rapidly leading to a local variation of the electron density from zero to a fraction of the critical density ($n_c = 6.875\times10^{21}$) in a time comparable to the probe pulse. As a simple estimate, if we assume a 100 μm thick (along the probe propagation axis) slab of gas changing its density of free electrons from zero (neutral gas) to a uniform value of $5\times10^{19}\text{cm}^{-3}$ we find a total change of optical path of almost λ_p. If this change occurs on a 60 fs time scale, large FVD will occur if probe pulse duration is comparable with or greater than 60 fs.

Moreover, if the probe pulse length is comparable to (or less than) its transit time in the region where the change of refractive index is occurring, the resulting interferometry map will be affected by probe transit effects. In fact, in our experimental configuration, the duration of the probe pulse can be significantly smaller than its transit time in the probed region. Also, the properties of this region are expected to change on a time-scale that is faster than the probe pulse duration. In these circumstances, transit effects become important and must be taken into account when analysing fringe patterns[17]. In general, the phase shift of the probe pulse due to propagation through a plasma is given by:

$$\Delta\varphi(x,y,T) = \frac{2\pi}{\lambda_p}\int_{-\infty}^{+\infty}\delta\mu\left(x,y,z,T+\frac{z}{c}\right)\,dz\ ,$$

where λ_p is the probe beam wavelength and $\delta\mu$ is the variation of the plasma refractive index (with respect to the vacuum), x and y are the axis in the image plane of the interferometer and z is the direction of propagation of the probe pulse.

This expression has been evaluated [17] assuming a cylindrical medium probed by a square probe pulse of duration τ. According to that model, transit time produces a region of FVD in the final interferometry map. Assuming that the change of refractive index under investigation occurs on a time scale much faster than the probe time, (i.e. a thin ionization front proceeds in the gas), than the FVD is uniform in a region around the image of the front and is given by:

$$V = V_o \frac{\sin(\mathrm{A})}{\mathrm{A}}$$

where $\mathrm{A} = \pi\delta\mu c\tau/\lambda_p$. We note that this relationship is independent of the diameter of the cylinder considered in the model. A correct evaluation of this formula requires a knowledge of the change of refractive index or, alternatively, the change of electron density. It is interesting to plot the visibility as a function of both parameters as displayed in Figure 9. According to this plot, a given change of the electron density identifies a minimum value of the probe pulse duration to produce a measured value of fringe visibility.

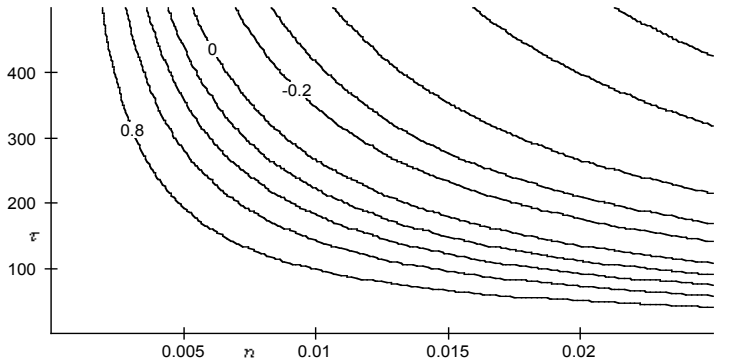

Figure 9. Calculated fringe visibility (normalized to 1) as a function of electron density (in units of the critical density at 400 nm) and probe pulse duration.

In our case, the gas can be assumed to be neutral before the arrival of the CPA pulse. After the CPA pump pulse, the electron density can be measured from the phase shift map (taken after propagation of the ionization front) through Abel inversion. In our experiment, the peak density is estimated to be 1.2×10^{20} cm^{-3}. Therefore, according to this analysis, a probe pulse shorter than 80 fs is required to preserve fringe visibility when changes of density of 1.2×10^{20} cm^{-3} take place.

Indeed, this simple model shows that, with the probe pulse duration of ≈130 fs used in our experiment, a significant reduction of fringe visibility can be expected. On the other hand, a quantitative comparison between measured and calculated values of the FVD should also include other features of the interaction like the actual temporal shape of the probe pulse. This task is beyond the aim of the present work. Here we stress that, according to the results described above, the observed FVD curves plotted in Figure 7 are closely related to the transient change of refractive index due ionization process. In other words, measurements of this kind can be effectively used to infer information on the dynamics of propagation of the ionization front in the gas. In fact,

our modeling of FVD implies that the depth of the ionization front must be shorter than the probe pulse duration. Therefore, provided that the observed FVD is entirely due to the mechanism described above, the longitudinal extent of the ionization front in our experiment is expected to be less than 40μm thick. Although in our case the relatively long probe pulse duration does not allow a more precise measurement to be achieved, it is important to point out that this is a quantitative information that cannot be obtained directly from the phase map due to the transit time effect. In fact, transit time will smooth steepness of the ionization front. The degree of this smoothing is related to the transverse size of the interaction region to be probed that, in our case, can be as large as several hundreds of μm. Therefore, direct analysis of interferograms without taking into account FVD, would lead to a large overestimation of the ionization front.

From a perspective point of view, it is clear that the use this analysis technique with of a very short probe pulse would enable a characterization of the shape and the scale-length of the ionization front with a micrometer-scale resolution.

CONCLUSIONS

We have presented experimental results concerning the propagation of an intense, ultra-fast laser pulse in a Helium gas-jet. Our high-quality, time resolved interferometric probe enabled us to detect gas ionization induced by the CPA pulse propagating in the gas. The loss of visibility of interferometric fringes, combined with probe transit-time analysis, was successfully used for the first time to track down the propagation of the ionization front in the gas. Our measurements show that ionization may occur in a less than 40μm thick layer that propagates in the gas at the speed of light. This result is limited by the duration of the probe pulse and could be significantly improved by using a shorter probe pulse. Our study demonstrates that visibility of fringes in an interferometric map can be profitably used for the investigation of spatial and temporal properties of propagation of CPA pulses in a gas.

ACKNOWLEDGMENTS

We would like to thank the staff of the SLIC laser facility for their invaluable and friendly support. We acknowledge support from the LASERLAB EUROPE Trans-national Access Programme. We thank W. Baldeschi and M. Voliani of the IPCF staff for their invaluable technical assistance. This work was partially supported by the joint INFN-CNR Project "Plasmon-X".

REFERENCES

1 Strickland D. and Mourou G., Opt. Comm., **56**, 219.(1985).
2 S.P.D. Mangles et al., Nature, **431**, 535 (2004); C.G.R. Geddes et al., Nature, **431**, 538 (2004); J. Faure et al., Nature, **431**, 541 (2004).
3 Y. Mairesse et al., Phys. Review Lett. 93 163901 (2004).
4 A. Rousse et al., Phys. Rev. Lett. 93 135005 (2004)
5 B. Walker et al., Phys. Rev. Lett. **73**, 1227 (1994).

6 D. Giulietti et al, Phys. Rev. Lett. **79**, 3194, 1997.
7 C.W. Siders et al., J. Opt. Soc. Am. B **13**, 300 (1996)
8 C.W. Siders et al., Phys. Rev. Lett. **87**, 263002 (2001)
9 L.A.Gizzi et al. Phys. Rev. E, 49, 5628 (1994); M.Borghesi et al., Phys. Rev. E 54 , 6769 (1996).
10 Giulietti D. et al, Phys. Plasmas, **9**, 3655, (2002).
11 M. Dunne et al., Phys. Rev. Lett. **72**, 1024 (1994); V. Malka et al., Phys. Rev. Lett. **79**, 2979 (1997).
12 M.J. Edwards et al., Phys. Rev. Lett. **87**, 085004 (2001).
13 M.G. Nomarsky, Phys. Rad. **16**, 95 (1955); R. Benattar, C. Popovics, and R. Siegel, Rev. Sci. Instrum. **50**, 1583 (1979); O.Willi, in *Laser-Plasma Interactions 4,* Proceedings of XXXV SUSSP, St. Andrews, 1988, edited by M. B. Hooper (SUSSP, Edimburgh, 1989).
14 M. Takeda, H. Ia, and S. Kobayashi, J. Opt. Soc. Am. **72**, 156, (1982); K.A. Nugent, Appl. Opt. **18**, 3101 (1985).
15 B. Walker et al., Phys. Rev. Lett., **73**, 1227 (1994).
16 P. Tomassini and A. Giulietti, Optics Comm. **199**, 143 (2001).
17 M. Galimberti, submitted to J. Optical Soc. Am. A (2005).